Original Article

Preoperative localization of single gland disease in primary hyperparathyroidism: a comparative study for preoperative localization with four-dimensional computed tomography, ultrasonography, and technetium-99m-sestamibi single-photon emission computed tomography

Ha-Nee Kwon[1]^, Hyeon-Su Kim[1]^, Sung-Chan Shin[1]^, Yong-Il Cheon[1]^, Bo Hyun Kim[2]^, Yun Kyung Jeon[2]^, Mijin Kim[2]^, Keunyoung Kim[3]^, Lee Hwangbo[4]^, Byung-Joo Lee[5]^

[1]Department of Otorhinolaryngology-Head and Neck Surgery, College of Medicine, Pusan National University and Biomedical Research Institute, Pusan National University Hospital, Busan, Republic of Korea; [2]Division of Endocrinology and Metabolism, Department of Internal Medicine, College of Medicine, Pusan National University and Biomedical Research Institute, Pusan National University Hospital, Busan, Republic of Korea; [3]Departments of Nuclear Medicine and Biomedical Research Institute, Pusan National University Hospital and School of Medicine, Pusan National University, Busan, Republic of Korea; [4]Departments of Radiology and Biomedical Research Institute, Pusan National University Hospital, Busan, Republic of Korea; [5]Department of Otorhinolaryngology-Head and Neck Surgery, Good Gang-An Hospital, Busan, Republic of Korea

Contributions: (I) Conception and design: BJ Lee, HN Kwon; (II) Administrative support: BH Kim, YK Jeon, M Kim, BJ Lee; (III) Provision of study materials or patients: BJ Lee, SC Shin; (IV) Collection and assembly of data: HN Kwon, HS Kim; (V) Data analysis and interpretation: HN Kwon, SC Shin, YI Cheon, L Hwangbo, K Kim; (VI) Manuscript writing: All authors; (VII) Final approval of manuscript: All authors.

Correspondence to: Byung-Joo Lee, MD, PhD. Department of Otorhinolaryngology-Head and Neck Surgery, Good Gang-An Hospital, 493 Suyeong-Ro, Suyeong-Gu, Busan 48265, Republic of Korea. Email: voiceleebj@gmail.com.

Background: Treatment guidelines for primary hyperparathyroidism (PHPT) recommend high-resolution neck ultrasonography (US), technetium-99m-sestamibi single-photon emission computed tomography (^{99m}Tc-sestamibi SPECT), and contrast-enhanced four-dimensional computed tomography (4D CT) as image evaluation methods. This study aimed to compare the sensitivity and accuracy of the three image evaluation methods recommended in the guidelines for patients with PHPT and evaluate the utility of 4D CT for preoperative localization in single gland disease.

Methods: A retrospective medical chart review was performed on 41 patients who underwent surgery for single gland disease at the Department of Otorhinolaryngology, Pusan National University Hospital, between January 2021 and March 2023. All the patients underwent preoperative US, ^{99m}Tc-sestamibi SPECT, and 4D CT. The location of the abnormal parathyroid lesion, removed during surgery and confirmed by postoperative pathological examination, was used as the reference standard. The sensitivity, specificity, and accuracy of the three imaging evaluations were assessed and compared to the reference standard location.

Results: The sensitivity, specificity, and accuracy of the imaging modalities were as follows: 4D CT, 95.1%, 98.4%, and 97.6%; US, 82.9%, 95.1%, and 92.1%; and ^{99m}Tc-sestamibi SPECT, 78.0%, 97.6%, and 92.7%, respectively. Furthermore, a total of nine cases were identified where accurate localization could not be achieved through US and ^{99m}Tc-sestamibi SPECT. The presence of coexisting thyroid lesions was significantly correlated with incorrect localization in preoperative US ($P<0.05$). The small volume of the parathyroid tumor was significantly associated with an increased rate of false-negatives using ^{99m}Tc-sestamibi

^ ORCID: Ha-Nee Kwon, 0000-0002-6965-9589; Hyeon-Su Kim, 0009-0000-5399-4545; Sung-Chan Shin, 0000-0003-2329-0648; Yong-Il Cheon, 0000-0003-0288-0542; Bo Hyun Kim, 0000-0001-9632-9457; Yun Kyung Jeon, 0000-0002-4319-5181; Mijin Kim, 0000-0002-1538-8859; Keunyoung Kim, 0000-0001-7555-3695; Lee Hwangbo, 0000-0002-1323-4450; Byung-Joo Lee, 0000-0001-7091-6688.

SPECT (P<0.05).
Conclusions: In the preoperative localization of abnormal parathyroid lesions, 4D CT demonstrated higher sensitivity and specificity than US and ^{99m}Tc-sestamibi SPECT. 4D CT can accurately localize abnormal parathyroid lesions, even in cases in which both US and ^{99m}Tc-sestamibi SPECT yielded incorrect localizations.

Keywords: Primary hyperparathyroidism (PHPT); parathyroidectomy; four-dimensional computed tomography (4D CT); technetium-99m-sestamibi single-photon emission computed tomography (^{99m}Tc-sestamibi SPECT); neck ultrasonography

Submitted Nov 07, 2024. Accepted for publication Feb 09, 2025. Published online Mar 26, 2025.
doi: 10.21037/gs-2024-482
View this article at: https://dx.doi.org/10.21037/gs-2024-482

Introduction

Primary hyperparathyroidism (PHPT) is characterized by the excessive secretion of parathyroid hormone (PTH), which typically results in hypercalcemia. In 85–90% of cases, a single benign parathyroid adenoma is the underlying cause, while carcinoma is extremely rare, accounting for less than 1% (1,2). PHPT, diagnosed based on clinical and biochemical criteria with elevated serum calcium and PTH levels, can lead to several complications, including increased risk of fracture due to osteoporosis, nephrolithiasis, cardiovascular disease, and peptic ulcer disease (2). The mainstay of treatment for PHPT is parathyroidectomy, and the indications for surgery are well-described in the latest guidelines (3).

Highlight box

Key findings
- Four-dimensional computed tomography (4D CT), neck ultrasonography (US), and technetium-99m-sestamibi single-photon emission computed tomography (^{99m}Tc-sestamibi SPECT) are valuable for localizing parathyroid adenoma(s) in primary hyperparathyroidism (PHPT).
- Among the localization modalities, 4D CT demonstrated the highest sensitivity and specificity.

What is known and what is new?
- US and ^{99m}Tc-sestamibi SPECT have been widely used for preoperative localization in patients with PHPT; however, each has limitations, particularly in cases with concurrent thyroid pathology or smaller parathyroid tumors.
- 4D CT outperformed US and ^{99m}Tc-sestamibi SPECT in sensitivity and specificity for PHPT localization, maintaining accuracy even when US and ^{99m}Tc-sestamibi SPECT yield negative results.
- While previous studies have compared these modalities individually, only few have directly compared all three together. Therefore, this study evaluated all three imaging modalities simultaneously, reaffirming the clear diagnostic advantages of 4D CT and providing a comprehensive comparison that may guide optimal imaging selection in clinical practice.

What is the implication, and what should change now?
- Given the superior localization accuracy of 4D CT, especially in challenging cases, it can be actively considered as a primary imaging modality for PHPT when US and ^{99m}Tc-sestamibi SPECT are inconclusive.

To ensure successful parathyroidectomy, precise localization of the abnormal parathyroid gland via thorough imaging is essential. This has enabled the adoption of minimally invasive parathyroidectomy as an alternative to the previously favored bilateral neck exploration, which was usually performed in the past. Although a recent systematic review did not conclusively show that minimally invasive parathyroidectomy is superior to bilateral neck exploration (4), it, including unilateral open parathyroidectomy, offers clear advantages in terms of reduced surgical risks and hospitalization, lower rates of complications, and lower patient costs (5-7).

Various methods have been proposed for the localization of the parathyroid adenoma(s) in patients with PHPT (8-10). According to current treatment guidelines for PHPT, high-resolution neck ultrasonography (US), integrated technetium-99m-sestamibi single-photon-emission computed tomography (^{99m}Tc-sestamibi SPECT), and contrast-enhanced four-dimensional computed tomography (4D CT) are recommended modalities for imaging evaluation (3). Therefore, this study compared the sensitivity and accuracy of these three imaging modalities for the evaluation of patients with single gland disease and assessed the usefulness of 4D CT compared with US and ^{99m}Tc-sestamibi SPECT. We present this article in accordance with the STARD reporting checklist (available at https://gs.amegroups.com/article/view/10.21037/gs-2024-482/rc).

Methods

Patients

A total of 41 patients who underwent surgery for single gland disease between January 2021 and March 2023 were enrolled in this study. All patients underwent surgery for the first time and were diagnosed with PHPT based on elevated blood PTH and calcium levels. Laboratory values, including blood PTH and calcium levels, were collected for all patients up to six months postoperatively. Preoperative imaging for all patients included neck US, ^{99m}Tc-sestamibi SPECT, and 4D CT. Patients diagnosed with single gland disease using all three imaging modalities and subsequently confirmed through postoperative pathology results were included in this study. The study was conducted in accordance with the Declaration of Helsinki (as revised in 2013). This retrospective study was approved by the Institutional Review Board of by the Pusan National University Hospital (No. 2302-010-124), and the requirement for informed consent was waived owing to the retrospective nature of the study.

High-resolution neck US

US examinations were performed by three endocrinologists with over 10 years of experience, using a US machine with a 7.5–15-MHZ linear transducer (Acuson S2000, SIEMENS Healthineers, Erlangen, Bayern, Germany; or Aplio i700, Canon Medical Systems, Otawara, Tochigi, Japan). The US was conducted first as part of the preoperative evaluation to ensure that the endocrinologists were blinded to the results of other imaging modalities. US examinations were performed with the patient in the supine position with the neck extended. Concomitant thyroid lesions (thyroiditis, multinodular goiter, or huge goiter) were evaluated simultaneously. Parathyroid lesions were characterized as abnormal when a well-circumscribed or slightly lobulated homogeneously echogenic mass was present in the expected area. When necessary, abnormal parathyroid glands were further evaluated using Doppler imaging, which showed polar vessels or rim-pattern vascularity.

^{99m}Tc-sestamibi SPECT

Dual-phase acquisitions of planar imaging, consisting of the anterior neck and upper thorax, were conducted at 20 minutes (early imaging) and 120 minutes (delayed imaging) after intravenous administration of a dose of 925 MBq (25 mCi) of ^{99m}Tc-sestamibi (Jubilant Radiopharma, Philadelphia, Pennsylvania, USA). The patients were placed in the supine position with their necks extended and their arms lowered alongside their bodies. Planar images were obtained using a dual-detector gamma camera (Symbia, SIEMENS Healthineers, Erlangen, Bayern, Germany), with static mode images obtained using a 256×256-pixel matrix and a 1.0× zoom factor at the previously mentioned predetermined time points (20 and 120 minutes). SPECT imaging was completed using a 128×128-pixel matrix, 1.0× zoom factor, and a slice thickness of 4.42 mm. Increased focal uptake and prolonged retention of ^{99m}Tc-sestamibi on a delayed 120-minute image was considered a positive finding for parathyroid lesions (11,12). All ^{99m}Tc-sestamibi SPECT images were interpreted by a board-certified nuclear medicine physician with over 10 years of experience in nuclear imaging, who was blinded to the results of other imaging modalities when interpreting the SPECT scans.

Contrast-enhanced 4D CT

Patients underwent 4D CT on a 64-row multirow detector CT scanner (Revolution Frontier, Revolution Apex, or Discovery CT 750 HD; GE HealthCare, Chicago, Illinois, USA). The images were reconstructed in the axial plane with a thickness of 1.25 mm. Nonenhanced images were obtained prior to injection of the contrast medium. After intravenous injection of 100 mL of contrast media, arterial, venous, and delayed-phase images were acquired at 30, 60, and 80 s, respectively. The 4D CT enhancement patterns (types A, B, and C), which indicate abnormal parathyroid glands, were classified according to the criteria described in a previous study (13). All 4D CT images were interpreted by a single radiologist with over 5 years of experience, who was blinded to the results of other imaging modalities. We then analyzed the clinical and pathological parameters according to the pattern of enhancement.

Surgery

Minimally invasive parathyroidectomy via a lateral approach or unilateral open parathyroidectomy was performed by

Table 1 Demographic and clinical characteristics of solitary primary hyperparathyroidism

Characteristics	Value (n=41)
Age (years)	58.9±10.1 [34–81]
Gender	
Male	6 (14.6)
Female	35 (85.4)
Tumor	
Size (cm)	1.60±0.64
Volume (cm^3)	5.60±5.16
Preoperative test	
PTH (pg/mL)	153.9±110.7
Calcium (mg/dL)	11.4±1.1
DXA T-score	−1.4±1.6
Location of abnormal parathyroid	
Right	
Upper	6 (14.6)
Lower	10 (24.4)
Left	
Upper	14 (34.2)
Lower	11 (26.8)

Data were presented as mean ± standard deviation [range] or n (%). DXA, dual-energy X-ray absorptiometry; PTH, parathyroid hormone.

two head and neck surgeons with >5 years of experience. The location of the abnormal parathyroid lesion, removed during surgery and confirmed pathologically, was used as the reference standard. Intraoperative frozen section biopsy was performed to confirm that the removed tissue was a parathyroid gland, and a subsequent pathologic confirmation was determined, diagnosing parathyroid adenoma, hyperplasia, or carcinoma. We obtained the dimensions of each parathyroid gland (length, width, and thickness) from the pathologic reports and calculated the corresponding semiaxes (a, b, and c). The gland volume was subsequently estimated using the ellipsoid volume formula: $V = \frac{4}{3}\pi abc$. All patients were followed for 6 months postoperatively.

Statistical analysis

Statistical analyses were performed using R version 4.2.2 (R Development Core Team, http://cran.r-project.org/). A normality test was conducted to assess the distribution of continuous variables prior to performing statistical comparisons. The characteristics of parathyroid lesions were compared among the three relative enhancement patterns on 4D CT. For these comparisons, continuous variables were analyzed using either one-way analysis of variance (ANOVA) or the Kruskal-Wallis test, depending on whether or not normality is satisfied. In contrast, categorical data were analyzed using the Chi-squared or Fisher's exact test. When comparing the two groups, continuous variables were analyzed using an independent *t*-test or Wilcoxon rank-sum test, whereas categorical data were analyzed using Fisher's exact test. The sensitivity, specificity, positive predictive value (PPV), negative predictive value (NPV), and accuracy of the three imaging modalities were determined based on the reference standard location. The 95% confidence intervals (CIs) for accuracy were calculated using the Clopper-Pearson exact method. Statistical significance was defined as $P<0.05$.

Results

Patients

Table 1 summarizes the demographic and clinical characteristics of the 41 patients who underwent surgery and were enrolled in this study. Thyroid surgery was performed concurrently in 12 patients. All patients who underwent concomitant surgery had coexisting conditions, including micropapillary thyroid cancer or large thyroid nodules. All parathyroid lesions were confirmed to be benign, with 28 cases identified as parathyroid adenoma and 13 as parathyroid hyperplasia. Blood PTH and calcium levels decreased postoperatively in all patients and were confirmed to be within the normal range at 6 months. None of them experienced postoperative vocal cord paralysis. Detailed information on the localization accuracy of US, 4D CT, and SPECT for all 41 cases, compared with surgical findings, is provided in Table S1.

Comparison of 4D CT, US, and ^{99m}TC-sestamibi SPECT

The sensitivity, specificity, and accuracy of the three

Table 2 Sensitivity, specificity, PPV, NPV, and accuracy of the three imaging modalities

Predictive performance values	4D CT		US		^{99m}Tc-sestamibi SPECT	
	Rate	95% CI	Rate	95% CI	Rate	95% CI
Sensitivity (%)	95.1	83.5–99.4	82.9	67.9–92.8	78.0	62.4–89.4
Specificity (%)	98.4	94.2–99.8	95.1	89.7–98.2	97.6	93.0–99.5
PPV (%)	95.1	83.5–99.4	85.0	70.2–94.3	91.4	76.9–98.2
NPV (%)	98.4	94.2–99.8	94.4	88.7–97.7	93.0	87.2–96.8
Accuracy (%)	97.6	93.9–99.3	92.1	86.8–95.7	92.7	87.6–96.2

4D CT, four-dimensional computed tomography; ^{99m}Tc-sestamibi SPECT, technetium-99m-sestamibi single-photon emission computed tomography; CI, confidence interval; NPV, negative predictive value; PPV, positive predictive value; US, ultrasonography.

Table 3 Combined performance of imaging modalities: sensitivity, specificity, PPV, NPV, accuracy

Predictive performance values	US + ^{99m}Tc-sestamibi SPECT	4D CT + ^{99m}Tc-sestamibi SPECT	US + 4D CT	US + 4DCT + ^{99m}Tc-sestamibi SPECT
Sensitivity (%)	95.1	97.6	100	100
Specificity (%)	98.4	99.2	100	100
PPV (%)	95.1	97.6	100	100
NPV (%)	98.4	99.2	100	100
Accuracy (%)	97.6	98.8	100	100

4D CT, four-dimensional computed tomography; ^{99m}Tc-sestamibi SPECT, technetium-99m-sestamibi single-photon emission computed tomography; NPV, negative predictive value; PPV, positive predictive value; US, ultrasonography.

imaging modalities were as follows: 4D CT, 95.1%, 98.4%, and 97.6%; US, 82.9%, 95.1%, and 92.1%; and ^{99m}Tc-sestamibi SPECT, 78.0%, 97.6%, and 92.7%, respectively (*Table 2*). Although 4D CT was unable to accurately determine abnormal parathyroid lesions in two cases out of the total, the sensitivity, specificity, and accuracy of 4D CT were the highest of the three imaging modalities.

We also analyzed the combined performance of the imaging modalities. The sensitivity, specificity, and accuracy for the combined modalities were as follows: US + ^{99m}Tc-sestamibi SPECT demonstrated 95.1%, 98.4%, and 97.6%, respectively; and ^{99m}Tc-sestamibi SPECT + 4D CT yielded 97.6%, 99.2%, and 98.8%, respectively (*Table 3*). Additionally, in the case of US + ^{99m}Tc-sestamibi SPECT, the localization results were found to be identical to those obtained when 4D CT was used alone (*Tables 2,3*). For US + 4D CT, correct localization of parathyroid adenomas was achieved in all 41 patients. Similarly, when all three imaging modalities (US + ^{99m}Tc-sestamibi SPECT + 4D CT) were used together, 100% accuracy was observed across all measures (*Table 3*).

Based on the enhancement patterns of parathyroid lesions using 4D CT, 19 cases (46.3%) were classified as type A, 20 cases (48.8%) as type B, and 2 cases (4.9%) as type C (*Table 4*). No comparison was observed between enhancement type and tumor volume, false-positive lesions, or parathyroid lesion location.

Incorrect localization cases in US and false negatives cases in ^{99m}Tc-sestamibi SPECT

Nine of the 41 cases examined using US exhibited incorrect localization. Preoperative PTH levels, tumor volume, and tumor location were not associated with incorrect localization. However, the presence of coexisting thyroid lesions, such as thyroiditis, multinodular goiter, or large thyroid nodule, was significantly associated with incorrect localization on US (P=0.03). Notably, all nine cases that showed incorrect localization on US were accurately localized on 4D CT (*Table 5*, *Figure 1*).

In ^{99m}Tc-sestamibi SPECT, 9 out of 41 cases showed false negatives. No significant association was found between

Table 4 Characteristics of primary hyperparathyroidism according to relative enhancement patterns

Characteristics	Type A (n=19)	Type B (n=20)	Type C (n=2)	P value
Age (years)	60.2±10.4	58.3±10.0	52.5±9.2	0.50
Gender				>0.99
Male	3 (15.8)	3 (15.0)	0	
Female	16 (84.2)	17 (85.0)	2 (100.0)	
Tumor				
Size (cm)	1.64±0.66	1.56±0.63	1.65±0.92	0.78
Volume (cm^3)	4.73±4.76	6.03±5.05	9.55±11.01	0.84
False positive lesion	0	2	0	0.54
Preoperative test				
PTH (pg/mL)	164.1±136.5	140.2±77.3	193.7±180.3	0.78
Calcium (mg/dL)	11.3±1.4	11.5±0.7	12.0±0.7	0.10
Location of parathyroid lesion				0.61
Right				
Upper	1 (5.3)	5 (25.0)	0	
Lower	5 (26.3)	5 (25.0)	0	
Left				
Upper	8 (42.1)	6 (30.0)	0	
Lower	5 (26.3)	4 (20.0)	2 (100.0)	

Data were presented as mean ± standard deviation, n (%), or n. PTH, parathyroid hormone.

preoperative PTH levels or location and false-negative results. However, it is worth noting that tumor volumes were statistically significantly smaller among patients with false negative results compared to those with true positive results (P=0.008). Notably, eight of the nine cases that showed false negatives on ^{99m}Tc-sestamibi SPECT were successfully localized on 4D CT (*Table 6*, *Figure 2*).

Of the two cases examined using 4D CT that exhibited incorrect localization, one was accurately localized on ^{99m}Tc-sestamibi SPECT. Notably, both cases were correctly localized on US (*Tables 5,6*).

Discussion

The imaging modalities utilized for the evaluation of PHPT include high-resolution US, integrated ^{99m}Tc-sestamibi SPECT, and 4D CT, alongside other modalities such as magnetic resonance imaging of the neck, integrated ^{18}F-choline/^{11}C-methionine positron emission tomography, angiographic selective venous sampling, and various combinations of sestamibi and thyroid scans (8-10). These combinations include sestamibi scans with I-123 thyroid scans with pertechnetate thyroid scans, either alone or with SPECT or SPECT/CT of the neck. These imaging modalities are used complementarily to maximize accuracy and precision in localizing parathyroid adenoma(s) through concordant imaging results (10). Among these methods, 4D CT, introduced in 2006, is one of the most recent (14). The characteristic findings of parathyroid adenoma on 4D CT are lower attenuation than those of the thyroid gland in the non-contrast enhancement phase, higher enhancement than the thyroid gland in the arterial phase, and faster washout than the thyroid gland in the delayed phase (15-17). However, this characteristic enhancement pattern is not the same for all abnormal parathyroid lesions (13).

Various methods have been proposed for the localization of the parathyroid gland in patients with PHPT, but the most commonly used methods are high-resolution neck US, ^{99m}Tc-sestamibi SPECT, and 4D CT (3). In a meta-analysis comparing these three imaging methods, the sensitivity and

Table 5 Clinical parameters according to ultrasonography outcomes

Characteristics	US incorrect (n=9)	US correct (n=32)	P value
Age (years)	58.8±5.4	58.9±11.1	0.96
Gender			>0.99
Male	1 (11.1)	5 (15.6)	
Female	8 (88.9)	27 (84.4)	
Tumor			
Size (cm)	1.67±0.47	1.58±0.69	0.73
Volume (cm^3)	5.86±5.61	5.53±5.11	0.87
Preoperative test			
PTH (pg/mL)	130.2±88.3	160.5±116.6	0.48
Calcium (mg/dL)	11.7±1.0	11.4±1.1	0.38
Coexisting thyroid lesion			0.03*
Presence	7 (77.8)	11 (34.4)	
Absence	2 (22.2)	21 (65.6)	
Location of parathyroid lesion			0.69
Right			
Upper	2 (22.2)	4 (12.5)	
Lower	1 (11.1)	9 (28.1)	
Left			
Upper	4 (44.4)	10 (31.2)	
Lower	2 (22.2)	9 (28.1)	
Localization of 4D CT			>0.99
Correct	9 (100.0)	30 (93.8)	
Incorrect	0	2 (6.2)	

Data were presented as mean ± standard deviation or n (%). *, P<0.05. 4D CT, four-dimensional computed tomography; PTH, parathyroid hormone; US, ultrasonography.

PPV were as follows: US, 76.1% (95% CI: 70.4–81.4%) and 93.2% (95% CI: 90.7–95.3%), respectively; ^{99m}Tc-sestamibi SPECT, 78.9% (95% CI: 64–90.6%) and 90.7% (95% CI: 83.5–96.0%), respectively; and 4D CT, 89.4% and 93.5%, respectively (18). In this study, the sensitivity and PPV of 4D CT were higher than those of US and ^{99m}Tc-sestamibi SPECT, consistent with the results of the aforementioned meta-analysis (18,19).

The sensitivity of CT used for the localization of parathyroid glands in another study was 73% (20). In subgroup analysis, the sensitivity of CT was higher when adding an additional contrast phase image rather than a single contrast phase (20). The 4D CT (three contrast phases with a non-contrast phase) performed in this study increased the accuracy of abnormal parathyroid localization compared to 2-phase CT with only one contrast phase; however, compared to 2-phase CT, 4D CT has the disadvantage of increasing a patient's exposure to ionizing radiation (20-22). Although 4D CT has relatively high radiation exposure, the risk of cancer due to 4D CT-related radiation exposure is very low (22). Although this study utilized the 4-phase protocol for 4D CT due to the undetermined optimal number of post-contrast phases, the 3-phase protocol is currently the most commonly used approach (10). Previous studies have demonstrated that the 3-phase protocol achieves comparable diagnostic accuracy

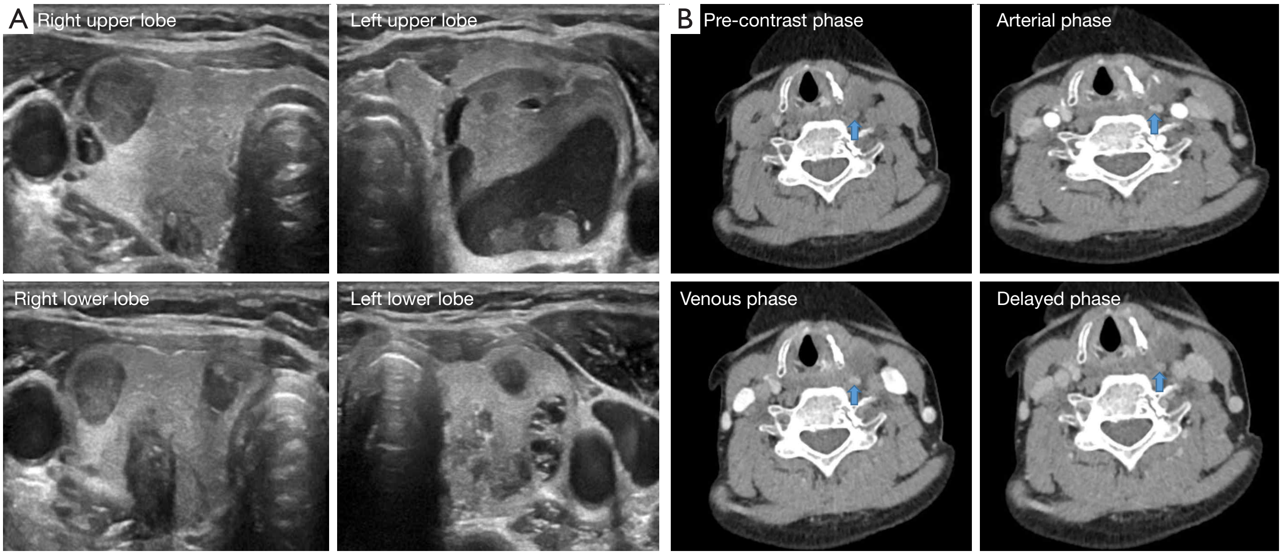

Figure 1 A representative case where localization was unattainable with US (A) but was successfully identified using 4D CT (B). Images of a 55-year-old woman with left superior parathyroid adenoma. (A) Due to the multinodular goiter, localization of abnormal parathyroid lesions using US was difficult. (B) 4D CT showing a parathyroid lesion (arrow) with type A enhancement characteristics. The lesion exhibits low attenuation during the pre-contrast phase and hyperattenuation during the arterial phase, after which the delayed-phase image shows a washout of contrast material with decreasing attenuation compared to the arterial phase. 4D CT, four-dimensional computed tomography; US, ultrasonography.

while reducing radiation exposure compared to the 4-phase protocol (8-10,15,20).

The 4D CT enhancement patterns for pathological parathyroid lesions can be classified into three previously described types (13). In our study, there were 19 type A cases (46.3%), 20 type B cases (48.8%), and 2 type C cases (4.9%). These results are somewhat different from those of a previous report, which reported 20% for type A, 57% for type B, and 22% for type C (13). Evaluating PHPT with 4D CT may have advantages over evaluation with 2-phase CT. In cases where type B pattern enhancement is observed on 4D CT, it can be easily diagnosed using a 2-phase scan. However, in the case of type C patterns, localization may be challenging with a 2-phase CT scan (13).

US is a noninvasive, inexpensive, and rapid method for tumor localization. It also has the advantage of being able to guide fine-needle aspiration or core biopsies of indeterminate lesions without exposing the patients to ionizing radiation (9,12). However, it has the disadvantage of being operator-dependent, and its sensitivity may decrease in the case of deep or hidden anatomical regions, exophytic thyroid nodules, or large multinodular goiter (8,9). In this study, the sensitivity, specificity, and accuracy of US were 82.9%, 95.1%, and 92.1%, respectively. Notably, a particularly high rate of incorrect localization has been observed in patients with concurrent thyroid lesions. Preoperative localization of the abnormal parathyroid gland was possible on 4D CT in all nine cases that were incorrectly diagnosed with US.

^{99m}Tc-sestamibi SPECT has the advantage of being less operator-dependent than US. It also has the advantage of excellent localization of ectopic parathyroid glands (8,9). However, false negatives may occur in cases with small parathyroid lesions or different washout times for parathyroid lesions (11,23). In our study, the sensitivity, specificity, and accuracy of ^{99m}Tc-sestamibi SPECT were 78.0%, 97.6%, and 92.7%, respectively, which are consistent with the results of other studies (24-26). There were nine cases in which ^{99m}Tc-sestamibi SPECT failed to localize abnormal parathyroid lesions, with false negatives significantly increasing for tumors with smaller volumes. This finding aligns with previous studies and can be attributed to the functional limitations of ^{99m}Tc-sestamibi SPECT. Specifically, its lower spatial resolution and reduced sensitivity to low radiotracer uptake in smaller or less metabolically active lesions likely contribute to its diminished performance in identifying small-volume lesions (8,12,23,27).

However, in eight of these nine cases, abnormal

Table 6 Clinical parameters according to SPECT outcomes

Characteristics	^{99m}Tc-sestamibi SPECT incorrect (n=9)	^{99m}Tc-sestamibi SPECT correct (n=32)	P value
Age (years)	57.0±12.4	59.4±9.5	0.53
Gender			>0.99
Male	1 (11.1)	5 (15.6)	
Female	8 (88.9)	27 (84.4)	
Tumor			
Size (cm)	1.23±0.56	1.70±0.63	0.051
Volume (cm^3)	2.69±2.69	6.42±5.41	0.008*
Preoperative test			
PTH (pg/mL)	172.7±174.6	148.6±88.5	0.70
Calcium (mg/dL)	10.8±1.1	11.6±1.0	0.04*
Location of parathyroid lesion			0.31
Right			
Upper	2 (22.2)	4 (12.5)	
Lower	1 (11.1)	9 (28.1)	
Left			
Upper	5 (55.6)	9 (28.1)	
Lower	1 (11.1)	10 (31.3)	
Localization of 4D CT			0.40
Correct	8 (88.9)	31 (96.9)	
Incorrect	1 (11.1)	1 (3.1)	

Data were presented as mean ± standard deviation or n (%). *, P<0.05. 4D CT, four-dimensional computed tomography; ^{99m}Tc-sestamibi SPECT, technetium-99m-sestamibi single-photon emission computed tomography; PTH, parathyroid hormone.

parathyroid gland localization was possible with 4D CT. Suh *et al.* (24) reported that the false negatives of 4D CT were significantly higher when the parathyroid tumor volume was smaller; however, in this study, precise preoperative localization was possible on 4D CT, even in the cases of small-size parathyroid lesions that were not detected on ^{99m}Tc-sestamibi SPECT. Among the methods for the preoperative localization of abnormal parathyroid lesions, US and parathyroid scintigraphy are the most common (12,15). We consider the two main disadvantages of 4D CT to be the risks associated with radiation exposure and the use of iodinated contrast media. The use of iodinated contrast media can induce allergic reactions and also poses a risk of contrast-induced nephropathy, making its use more challenging in patients with renal dysfunction. However, 4D CT has higher sensitivity and accuracy than US and ^{99m}Tc-sestamibi SPECT for preoperative localization of abnormal parathyroid lesions (18). Additionally, in our study, in cases of incorrect localization on US or ^{99m}Tc-sestamibi SPECT, preoperative localization was possible on 4D CT in most cases. As such, the number of radiologists who want to use 4D CT as a first-line study for parathyroid localization is gradually increasing (15).

There are several limitations to this study. First, its retrospective nature and small sample size limit the statistical power of the findings. As a result, there is potential statistical bias, and no statistically significant differences were observed in the CI analysis. Although including patients with multiglandular disease (MGD) could have increased the sample size, we included only patients with single-gland disease due to the lower incidence of PHPT in South Korea (28). Consequently, the exclusion of MGD cases prevented validation of the efficacy and may have introduced selection bias. Second, the findings

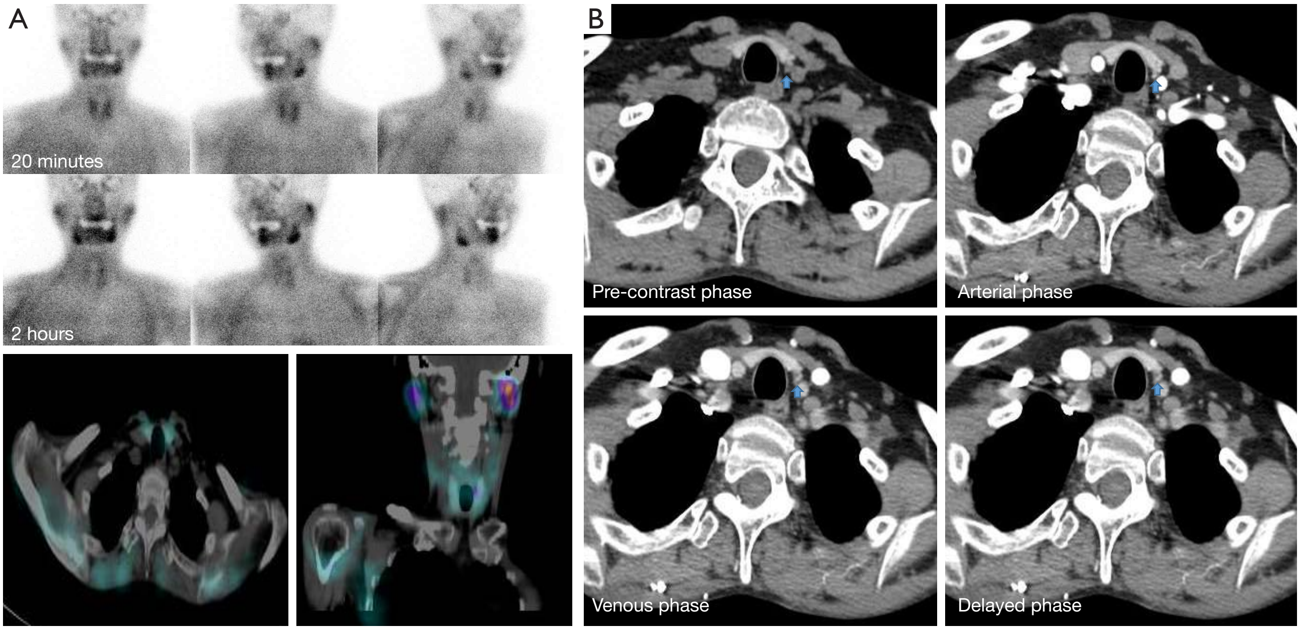

Figure 2 A representative case where localization failed using ^{99m}Tc-sestamibi SPECT (A), yet effectively identified by 4D CT (B). Images of a 58-year-old woman with a left inferior parathyroid lesion. (A) ^{99m}Tc-sestamibi SPECT does not show abnormal findings and is considered normal. (B) On 4D CT, a parathyroid lesion (arrow) was observed with type B enhancement characteristics. The attenuation of the lesion was lower than that of the adjacent thyroid gland during the pre-contrast phase. The arterial phase image demonstrates that the lesion has a similar attenuation as the adjacent thyroid gland, and the lesion shows a faster washout of contrast material than the adjacent thyroid gland during the delayed phase. 4D CT, four-dimensional computed tomography; ^{99m}Tc-sestamibi SPECT, technetium-99m-sestamibi single-photon emission computed tomography.

are based on data from a single institution, which may restrict the generalizability of the results to other clinical settings or populations. To address this limitation, larger multicenter studies are necessary to validate our findings and provide a more comprehensive understanding of the diagnostic performance of 4D CT. Third, this study utilized the 4-phase protocol for 4D CT, which does not reflect the current standard. The 3-phase protocol is now more commonly adopted as it achieves similar diagnostic accuracy with reduced radiation exposure (8-10,15,20). Future research employing the 3-phase protocol will help align findings with contemporary clinical practices. Fourth, while this study confirms similar findings to prior research (9), it does not present novel results. However, it adds value by simultaneously comparing the performance of three imaging modalities (US, 4D CT, and ^{99m}Tc-sestamibi), unlike most previous studies, which have typically compared individual or two modalities. Finally, clinical practice often relies on a combined approach using multiple imaging modalities rather than a single modality. The integration of imaging results through multidisciplinary expert panels is essential for accurate localization and optimal clinical decision-making. Future studies should evaluate the diagnostic value of combining modalities and emphasize the role of expert consensus in improving patient outcomes.

Conclusions

In conclusion, 4D CT demonstrated higher sensitivity and specificity than US and ^{99m}Tc-sestamibi SPECT for the preoperative localization of abnormal parathyroid lesions. However, further large-scale, multicenter studies are necessary to validate the diagnostic accuracy of 4D CT and clearly define its role. Despite this, 4D CT serves as a valuable tool for the preoperative evaluation of patients with single gland disease.

Acknowledgments

None.

Footnote

Reporting Checklist: The authors have completed the STARD reporting checklist. Available at https://gs.amegroups.com/article/view/10.21037/gs-2024-482/rc

Data Sharing Statement: Available at https://gs.amegroups.com/article/view/10.21037/gs-2024-482/dss

Peer Review File: Available at https://gs.amegroups.com/article/view/10.21037/gs-2024-482/prf

Funding: This study was supported by a National Research Foundation of Korea (NRF) grant funded by the Korean government (MSIT) (No. NRF 2022R1A2C2006697).

Conflicts of Interest: All authors have completed the ICMJE uniform disclosure form (available at https://gs.amegroups.com/article/view/10.21037/gs-2024-482/coif). The authors have no conflicts of interest to declare.

Ethical Statement: The authors are accountable for all aspects of the work in ensuring that questions related to the accuracy or integrity of any part of the work are appropriately investigated and resolved. The study was conducted in accordance with the Declaration of Helsinki (as revised in 2013) and approved by the Institutional Review Board of the Pusan National University Hospital (No. 2302-010-124). The requirement for informed consent was waived owing to the retrospective nature of the study.

References

1. Walker MD, Silverberg SJ. Primary hyperparathyroidism. Nat Rev Endocrinol 2018;14:115-25.
2. Wilhelm SM, Wang TS, Ruan DT, et al. The American Association of Endocrine Surgeons Guidelines for Definitive Management of Primary Hyperparathyroidism. JAMA Surg 2016;151:959-68.
3. Bilezikian JP, Khan AA, Silverberg SJ, et al. Evaluation and Management of Primary Hyperparathyroidism: Summary Statement and Guidelines from the Fifth International Workshop. J Bone Miner Res 2022;37:2293-314.
4. Ahmadieh H, Kreidieh O, Akl EA, et al. Minimally invasive parathyroidectomy guided by intraoperative parathyroid hormone monitoring (IOPTH) and preoperative imaging versus bilateral neck exploration for primary hyperparathyroidism in adults. Cochrane Database Syst Rev 2020;10:CD010787.
5. Kunstman JW, Udelsman R. Superiority of minimally invasive parathyroidectomy. Adv Surg 2012;46:171-89.
6. Laird AM, Libutti SK. Minimally Invasive Parathyroidectomy Versus Bilateral Neck Exploration for Primary Hyperparathyroidism. Surg Oncol Clin N Am 2016;25:103-18.
7. Rawat A, Grover M, Kataria T, et al. Minimally Invasive Parathyroidectomy as the Surgical Management of Single Parathyroid Adenomas: A Tertiary Care Experience. Indian J Otolaryngol Head Neck Surg 2023;75:271-7.
8. Zarei A, Karthik S, Chowdhury FU, et al. Multimodality imaging in primary hyperparathyroidism. Clin Radiol 2022;77:e401-16.
9. Bunch PM, Kelly HR. Preoperative Imaging Techniques in Primary Hyperparathyroidism: A Review. JAMA Otolaryngol Head Neck Surg 2018;144:929-37.
10. Expert Panel on Neurological Imaging; Zander D, Bunch PM, et al. ACR Appropriateness Criteria® Parathyroid Adenoma. J Am Coll Radiol 2021;18:S406-22.
11. Kuzminski SJ, Sosa JA, Hoang JK. Update in Parathyroid Imaging. Magn Reson Imaging Clin N Am 2018;26:151-66.
12. Strauss SB, Roytman M, Phillips CD. Parathyroid Imaging: Four-dimensional Computed Tomography, Sestamibi, and Ultrasonography. Neuroimaging Clin N Am 2021;31:379-95.
13. Bahl M, Sepahdari AR, Sosa JA, et al. Parathyroid Adenomas and Hyperplasia on Four-dimensional CT Scans: Three Patterns of Enhancement Relative to the Thyroid Gland Justify a Three-Phase Protocol. Radiology 2015;277:454-62.
14. Rodgers SE, Hunter GJ, Hamberg LM, et al. Improved preoperative planning for directed parathyroidectomy with 4-dimensional computed tomography. Surgery 2006;140:932-40; discussion 940-1.
15. Hoang JK, Williams K, Gaillard F, et al. Parathyroid 4D-CT: Multi-institutional International Survey of Use and Trends. Otolaryngol Head Neck Surg 2016;155:956-60.

16. Beland MD, Mayo-Smith WW, Grand DJ, et al. Dynamic MDCT for localization of occult parathyroid adenomas in 26 patients with primary hyperparathyroidism. AJR Am J Roentgenol 2011;196:61-5.
17. Gafton AR, Glastonbury CM, Eastwood JD, et al. Parathyroid lesions: characterization with dual-phase arterial and venous enhanced CT of the neck. AJNR Am J Neuroradiol 2012;33:949-52.
18. Cheung K, Wang TS, Farrokhyar F, et al. A meta-analysis of preoperative localization techniques for patients with primary hyperparathyroidism. Ann Surg Oncol 2012;19:577-83.
19. Kattar N, Migneron M, Debakey MS, et al. Advanced Computed Tomographic Localization Techniques for Primary Hyperparathyroidism: A Systematic Review and Meta-analysis. JAMA Otolaryngol Head Neck Surg 2022;148:448-56.
20. Kluijfhout WP, Pasternak JD, Beninato T, et al. Diagnostic performance of computed tomography for parathyroid adenoma localization; a systematic review and meta-analysis. Eur J Radiol 2017;88:117-28.
21. Noureldine SI, Aygun N, Walden MJ, et al. Multiphase computed tomography for localization of parathyroid disease in patients with primary hyperparathyroidism: How many phases do we really need? Surgery 2014;156:1300-6; discussion 13006-7.
22. Mahajan A, Starker LF, Ghita M, et al. Parathyroid four-dimensional computed tomography: evaluation of radiation dose exposure during preoperative localization of parathyroid tumors in primary hyperparathyroidism. World J Surg 2012;36:1335-9.
23. Ozkaya M, Elboga U, Sahin E, et al. Evaluation of conventional imaging techniques on preoperative localization in primary hyperparathyroidism. Bosn J Basic Med Sci 2015;15:61-6.
24. Suh YJ, Choi JY, Kim SJ, et al. Comparison of 4D CT, ultrasonography, and 99mTc sestamibi SPECT/CT in localizing single-gland primary hyperparathyroidism. Otolaryngol Head Neck Surg 2015;152:438-43.
25. Pereira C. Role of Single-Photon Emission Computerised Tomography Versus Ultrasonography or 4D-Computed Tomography in the Management of Primary Hyperparathyroidism. Cureus 2022;14:e29015.
26. Yeh R, Tay YD, Tabacco G, et al. Diagnostic Performance of 4D CT and Sestamibi SPECT/CT in Localizing Parathyroid Adenomas in Primary Hyperparathyroidism. Radiology 2019;291:469-76.
27. Kairemo K, Jessop AC, Vija AH, et al. A Prospective Comparative Study of Using Ultrasonography, 4D-CT and Parathyroid Dual-Phase Scintigraphy with SPECT in Patients with Primary Hyperparathyroidism. Diagnostics (Basel) 2021;11:2006.
28. Kim JK, Chai YJ, Chung JK, et al. The prevalence of primary hyperparathyroidism in Korea: a population-based analysis from patient medical records. Ann Surg Treat Res 2018;94:235-9.

Cite this article as: Kwon HN, Kim HS, Shin SC, Cheon YI, Kim BH, Jeon YK, Kim M, Kim K, Hwangbo L, Lee BJ. Preoperative localization of single gland disease in primary hyperparathyroidism: a comparative study for preoperative localization with four-dimensional computed tomography, ultrasonography, and technetium-99m-sestamibi single-photon emission computed tomography. Gland Surg 2025;14(3):305-316. doi: 10.21037/gs-2024-482

Supplementary

Table S1 Summary of imaging results and surgical findings in 41 cases

No.	US	SPECT	4D CT	Reference (surgery)
1	Left lower	Non confirm	Left upper	Left upper
2	Non confirm	Non confirm	Left upper	Left upper
3	Non confirm	Right upper	Right upper	Right upper
4	Left lower	Left lower	Left lower	Left lower
5	Left upper	Non confirm	Left upper	Left upper
6	Left lower	Left lower	Non confirm	Left lower
7	Left upper	Left upper	Left upper	Left upper
8	Right lower	Non confirm	Right upper	Right lower
9	Left upper	Non confirm	Left upper	Left upper
10	Left lower	Left upper	Left upper	Left upper
11	Right lower	Right lower	Right lower	Right lower
12	Left upper	Left upper	Left upper	Left upper
13	Right lower	Right lower	Right lower	Right lower
14	Right lower	Right upper	Right upper	Right upper
15	Left lower	Left lower	Left lower	Left lower
16	Left lower	Non confirm	Left lower	Left lower
17	Left upper	Left upper	Left upper	Left upper
18	Left upper	Left upper	Left upper	Left upper
19	Left upper	Left upper	Left upper	Left upper
20	Left upper	Left upper	Left upper	Left upper
21	Right lower	Right lower	Right lower	Right lower
22	Left lower	Left lower	Left lower	Left lower
23	Left upper	Left upper	Left upper	Left upper
24	Left lower	Left lower	Left lower	Left lower
25	Left lower	Right lower	Right lower	Right lower
26	Right lower	Right lower	Right lower	Right lower
27	Non confirm	Left Lower	Left Lower	Left Lower
28	Left upper	Left lower	Left lower	Left lower
29	Right upper	Non confirm	Right upper	Right upper
30	Right lower	Right lower	Right lower	Right lower
31	Right lower	Right lower	Right lower	Right lower
32	Right upper	Non confirm	Right upper	Right upper
33	Left lower	Left lower	Left lower	Left lower
34	Left upper	Left upper	Left upper	Left upper
35	Left lower	Left lower	Left lower	Left lower
36	Right upper	Right upper	Right upper	Right upper
37	Right lower	Right lower	Right lower	Right lower
38	Left lower	Left lower	Left lower	Left lower
39	Left upper	Non confirm	Left upper	Left upper
40	Right upper	Right upper	Right upper	Right upper
41	Right lower	Right lower	Right lower	Right lower

4D CT, four-dimensional computed tomography; SPECT, single-photon emission computed tomography; US, ultrasonography.

https://dx.doi.org/10.21037/gs-2024-482